IEEE Access
Multidisciplinary ⋮ Rapid Review ⋮ Open Access Journal

Received 22 July 2024, accepted 4 August 2024, date of publication 13 August 2024, date of current version 22 August 2024.

Digital Object Identifier 10.1109/ACCESS.2024.3443089

RESEARCH ARTICLE

Theory of Run-Length Domain Modal Decomposition for Assessing Dynamic Errors in Electricity Meter

RUIMING YUAN[1], (Associate Member, IEEE), WENWEN LI[1], GUOXING WANG[1], DI WU[2], SHIYU XIE[2], AND XUEWEI WANG[2]

[1]Metrology Center, State Grid Jibei Electric Power Company Ltd., Beijing 100045, China
[2]College of Information Science and Technology, Beijing University of Chemical Technology, Beijing 100029, China

Corresponding author: Wenwen Li (821328633@qq.com)

This work was supported by the State grid corporation of China Technology Project in Beijing, China under Grant 5700-202211214A-1-1-ZN.

ABSTRACT In scenarios involving photovoltaic power generation and electrical dynamic loads, complex electricity metering signals often exhibit strong randomness and rapid fluctuations. These characteristics frequently lead to substantial errors in electricity metering, thereby affecting fair and equitable energy transactions. This paper presents a novel modal decomposition theory in the run-length domain. Such a theory is developed to map signals from the amplitude domain to run sequences in the run-length domain. Subsequently, it decomposes signals into a quasi-steady, slowly varying mode, and another dynamic, rapidly fluctuating mode, facilitating the extraction of sensitive characteristics over prolonged durations. Furthermore, the paper proposes characteristics representation method for complex electricity metering signals by constructing parameters and characteristic functions in the run-length domain. Additionally, the paper specifically extracts sensitive characteristics for photovoltaic complex electricity metering signals using the modal decomposition theory in the run-length domain. Finally, experimental validation is conducted to elucidate the impact of these sensitive characteristics on electricity meter errors with the maximum dynamic error observed at −15.53%.

INDEX TERMS Characteristic extraction, dynamic error in electricity meter, electrical energy metering, modal decomposition, photovoltaic new energy.

I. INTRODUCTION

With the advent of new power systems, the utilization of renewable energy sources like wind and photovoltaic power is steadily rising across numerous countries. However, high-power electric loads, such as electric high-speed railways and electric arc furnaces, present unique challenges due to their complex and dynamic nature, characterized by significant randomness, large fluctuations, and rapid variations.

At present, power systems in many countries worldwide are undergoing a transition towards clean, low-carbon, and intelligent solutions. The share of new power sources, such as wind power and photovoltaic power, along with electrical dynamic loads, is steadily increasing within the power grid [1], [2].

In recent years, it has been observed that fast variations in load current and power, occurring in both photovoltaic power systems and electrical dynamic loads, can induce significant errors (up to 40%) in electricity metering [3], [4]. Consequently, these fast current variations can have a considerable impact on financial settlements between energy suppliers and consumers. Load current and power, when combined with voltage, are referred to as 'complex dynamic electricity signals' (hereafter referred to as CD electricity signals) when they exhibit significant randomness and rapid variations across a wide range.

The associate editor coordinating the review of this manuscript and approving it for publication was Mohamed Kheir.

In the past decades, significant interest has been shown by many researchers in analyzing the error-inducing characteristics of CD electricity signals. Numerous analysis methods and findings have been published, primarily focusing on two aspects: (1) short-duration harmonic characteristic extraction, and (2) short-duration waveform characteristic extraction.

In the domain of short-duration harmonic characteristic extraction, numerous frequency-domain methods have been proposed, including the interpolation FFT method [5], [6], [7], the windowed interpolation FFT method [8], [9], self-convolution window FFT method [10], [11], and others [12], [13], [14]. These methods involve extracting local characteristics of fundamental and harmonic amplitudes, frequencies, and phases within a 10-second time duration. One of objectives is to evaluate the influence of harmonic characteristics on electricity meter accuracy.

In the domain of short-duration waveform characteristics extraction, several time-domain methods have been reported in the literature. For instance, in the case of low-power pumps, two fast-varying characteristics—local waveform peak and fluctuation range—are built from one-cycle current to analyze the impact of fast-varying local waveform on electricity meters [15]. Similarly, for LED lamps, low-power dimmers, and fluorescent lamps, three fast-varying waveform characteristics—local waveform rise time, rise rate, and peak slope—are extracted from two-cycle local current to investigate their impact on electricity meter errors [16], [17].

However, in both photovoltaic power and dynamic loads scenarios, what fast fluctuation characteristics of current amplitude can induce electricity metering errors has not been completely understand until now, especially characteristics lasting more than 30 minutes. And investigating new characteristics analyzing method and furthermore finding important characteristics have become a challenging work for determine test signal condition during evaluating the errors of the electricity meters.

Summarizing the above discussion, the aforementioned short-duration characteristics extraction methods can successfully extract several local characteristics of CD electricity signals within a few power frequency cycles. However, they have overlooked the evolution of local characteristics during prolonged periods exceeding 30 minutes. Therefore, they face challenges in extracting the ''sensitive characteristics'' which induce significant errors in electricity metering.

The main contributions of the paper are as follows: 1) A theory of mapping CD electricity signals from the amplitude domain to the run-length domain was proposed, 2) A run-length domain modal decomposition (RMD) method was proposed for extracting truncated curve in signal amplitude, 3) Novel characteristic functions were constructed in the run-length domain to solve extraction of sensitive characteristics which induce significant errors in electricity metering. The results obtained in this study can be used as the key characteristic information of dynamic test signals for type testing and for updating the IEC standards for electricity meter.

TABLE 1. Technical jargons and explanations.

Number	Technical jargons	Explanations
1	Complex dynamic electricity signals (CD electricity signals)	The instantaneous current on the secondary side of the Current Transformer and the instantaneous voltage on the secondary side of the Voltage Transformer, utilized for electricity metering, exhibit strong randomness and rapid fluctuations across a wide range.
2	Sensitive characteristics	The characteristics of current variation that induce significant errors in electricity metering
3	Ascending run	A segment of the current amplitude that exceeds the truncation curve and maintains continuous intervals.
4	The length of the ascending run	The number of power frequency cycles that the ascending run lasts.
5	Descending run	A segment of the current amplitude that falls below the truncation curve and maintains continuous intervals.
6	The length of the descending run	The number of power frequency cycles that the descending run lasts.
7	Run pair	A run pair consists of an ascending run followed by an adjacent descending run.
8	The length of the run pair.	The number of power frequency cycles that the run pair lasts.
9	Run-length domain	The domain consisting of ascending runs, descending runs and run pairs.
10	Quasi-steady term	The slowly varying mode decomposed from the randomly fast-varying signal.
11	Dynamic term	The rapidly varying mode decomposed from the randomly fast-varying signal.
12	Run fluctuation mode	The mode divided based on the duration of the run's fluctuation.
13	Short-Time fluctuation mode	The mode duration that lasts 1-4s.
14	Long-Time fluctuation mode	The mode duration that lasts 4-60s.
15	Ultra-Long-Time fluctuation mode	The mode duration that lasts 60-300s.
16	OOK test signal	The test signal consisting of on-off-keying signal.

The remainder of this paper is organized as follows. In Section V, Applying the RMD decomposition and characteristic extraction theory, we validate a case of photovoltaic (PV) new energy CD electricity signals, to analyze and extract their sensitive characteristics. In Section VI, based on extracted characteristics, OOK dynamic test signal model parameters are determined to evaluate the Impact of the Sensitive characteristics on the Dynamic Errors of Electricity Meters. These test findings provide valuable insights for supplementing international electricity meter standard test method.

To make the paper more accessible to readers from diverse backgrounds, the following Table 1 explains key technical jargons proposed in the paper.

II. RUN-LENGTH DOMAIN MAPPING THEORY OF CD ELECTRICITY SIGNALS

A. AMD CHARACTERISTICS ANALYSIS OF DYNAMIC CURRENT

Under actual operating conditions, the amplitude of electrical energy metering currents and power signals exhibits characteristics of strong randomness, rapid fluctuations. In this

section, a signal model is established using stochastic processes.

According to stochastic processes theory, let e denote the amplitude of CD electricity signals, E denote the sample space of signal amplitudes, and $T = \{n', n' = 1, 2, \ldots N\}$ denote the discrete time set. Then, CD electricity signals can be represented as a stochastic process $\{\tilde{X}(n', e), n' \in T, e \in E\}$. Let each signal $\tilde{x}(n')$ collected be a sample of this stochastic process. The general model for a stochastic CD electricity signal be expressed as follows:

$$\begin{aligned}\tilde{x}(n') &= \sum_{q=1}^{Q} \tilde{A}_q(n')s(n') + N(n') \\ &= \sum_{q=1}^{Q} \tilde{A}_q(n')\sin(\omega_q n' + \varphi_q(n')) + N(n') \end{aligned} \tag{1}$$

where, "$\sim$" represents a random function, n'=0,1,2$\cdots$ denotes discrete time, q represents the harmonic order, ω_q signifies the angular frequency, $\varphi_q(n')$ denotes the initial phase of each harmonic, reflecting the fundamental and harmonic characteristics of the current. $\tilde{A}_q(n')$ represents the amplitude-modulated signal, indicating the strong stochastic and non-stationary amplitude variations of the signal, following a certain probability distribution. $s(n')$ denotes the modulated signal, reflecting the various harmonic components formed by multiple signals. $N(n')$ represents additive noise, reflecting the noise components in the CD electricity signals.

B. CONSTRUCTING TIME SERIES MODELS FOR CD ELECTRICITY SIGNALS

In consideration of (1) depicting the stochastic signal model, this paper employs the Short-Time Fourier Transform time-frequency analysis method to extract the time series of amplitudes for the fundamental frequency and harmonics of the electrical energy signal as follows:

$$\begin{aligned}\tilde{X}(n, q) &= \sum_{n'=1}^{M_s-1} \tilde{x}(n')g(n' - nM_s)e^{-j2\pi n'q/M_s} \\ &= \{\tilde{X}(0, q), \tilde{X}(1, q), \ldots \tilde{X}(n, q), \ldots\} \end{aligned} \tag{2}$$

where, $M_s = \lfloor f_s/f_1 \rfloor$ represents the length of the window function, f_1 denotes the fundamental frequency, and $n = \lfloor n'/M_s \rfloor$ represents the ordinal number of the power frequency cycle. When representing voltage and current signals, $\tilde{X}(n, q)$ takes the values of $\tilde{U}_k^d(n, q)$ and $\tilde{I}_k^d(n, q)$ respectively.

According to the algorithm in (2), voltage amplitudes $\tilde{U}_k^d(n, q)$ and current amplitudes $\tilde{I}_k^d(n, q)$ of each harmonic are extracted, and a dynamic electrical energy metering voltage and current signal time series model is established as follows:

$$\tilde{u}_k^d(n') = \sum_{q=1}^{Q} \tilde{U}_k^d(n, q)\sin(\omega_q n' + \varphi_{kq}^u(n')) + N^u(n') \tag{3}$$

$$\tilde{i}_k^d(n') = \sum_{q=1}^{Q} \tilde{I}_k^d(n, q)\sin(\omega_q n' + \varphi_{kq}^i(n')) + N^i(n') \tag{4}$$

where, superscript d indicates that the signal is dynamic, subscript k represents the A, B, C three phases, n denotes the power frequency cycle number, u and i respectively represent voltage and current, and $\tilde{U}_k^d(n, q)$, $\tilde{I}_k^d(n, q)$ denote the amplitudes of the fundamental and harmonic components. When the distortion of grid voltage and current is small, $q = 1$ can be set to simplify the voltage fundamental amplitude $\tilde{U}_k^d(n, 1)$ and the current fundamental amplitude $\tilde{I}_k^d(n, 1)$ as $U_k^d(n)$ and $I_k^d(n)$.

In power grids, the variation of the amplitude of complex dynamic current fundamental exhibits strong randomness and rapid fluctuations, which are the primary factors affecting energy metering accuracies. Conversely, the dynamic variation of voltage fundamental amplitude demonstrates weak randomness and slow minor fluctuations characteristics, rendering its impact on electricity metering accuracies negligible. Therefore, the following sections focus on the run-length domain mapping, modal decomposition, and characteristic extraction for the complex dynamic current fundamental amplitude.

C. RUN MAPPING THEORY FOR TIME SERIES OF COMPLEX DYNAMIC CURRENTS

In order to address the challenge of simultaneously extracting the rapid changing characteristics of complex dynamic current signals within local intervals and the evolving characteristics of these characteristics over prolonged durations, this section investigates a run mapping theory, to maps the signals from the amplitude domain to run sequence in run-length domain, making it easier to extract local characteristics.

1) MAPPING CURRENT AMPLITUDE INTO RUN SEQUENCE IN RUN-LENGTH DOMAIN

For the complex dynamic current fundamental amplitude $I_k^d(n)$, the slowly varying trend component $I_k^c(n)$ is selected as the truncation curve. When $I_k^c(n)$ exhibits a certain changing trend over time and satisfies the continuous interval with the same attribute given by the following equation:

$$\begin{cases} I_k^d(n_l^+) = I_k^c(n_l^+); I_k^d(n_l^+ + \tau_l^+) \le I_k^c(n_l^+ + \tau_l^+) \\ I_k^d(n_l^+ + i) > I_k^c(n_l^+ + i); i = 1, 2, \ldots, (\tau_l^+ - 1) \end{cases} \tag{5}$$

Then, the current amplitude $I_k^d(n)$ within the continuous interval given by (5) is mapped into an ascending run.

$$\tilde{R}(n_l^+, \tau_l^+) = \left\{I_k^d(n_l^+), I_k^d(n_l^+ + 1), \ldots, I_k^d(n_l^+ + \tau_l^+)\right\} \tag{6}$$

where, $l = 1, 2, \ldots$ represents the run number, the parameter n_l^+ represents the power frequency cycle number corresponding to the starting point of the ascending run, the parameter τ_l^+ is defined as the length of the ascending run, and $\tilde{R}(n_l^+, \tau_l^+)$ denotes the l-th ascending run in the run-length

domain. Similarly, when $I_k^d(n)$ satisfies the continuous interval with the same attributes given by the following equation on the time scale:

$$\begin{cases} I_k^d(n_l^-) = I_k^c(n_l^-); I_k^d(n_l^- + \tau_l^-) \geq I_k^c(n_l^- + \tau_l^-) \\ I_k^d(n_l^- + i) < I_k^c(n_l^- + i); i = 1, 2, \ldots, (\tau_l^- - 1) \end{cases} \tag{7}$$

Then, the current amplitude $I_k^d(n)$ within the continuous interval given by (7) is mapped to the l-th descending run immediately following the ascending run $\tilde{R}(n_l^+, \tau_l^+)$.

$$\tilde{R}(n_l^-, \tau_l^-) = \left\{ I_k^d(n_l^-), I_k^d(n_l^- + 1), \ldots, I_k^d(n_l^- + \tau_l^-) \right\} \tag{8}$$

where, the parameter $n_l^- = n_l^+ + \tau_l^+$ represents the starting number of power frequency cycle included in $\tilde{R}(n_l^-, \tau_l^-)$, and the parameter τ_l^- is defined as the length of the descending run. In the text, both ascending and descending runs are collectively referred to as run $\tilde{R}(n_l^\pm, \tau_l^\pm)$. When $n_l^\pm, \tau_l^\pm$ is taken, it represents an ascending run from n_l^+, τ_l^+, and when n_l^-, τ_l^- is taken, it represents a descending run.

2) BASIC PARAMETERS OF THE RUN-LENGTH DOMAIN

In order to decompose the runs of current amplitude and extract run characteristics, this section first provides the definition of basic parameters in the run-length domain.

Definition 1: Run Pair $\tilde{R}(n_l, \tau_l)$

An ascending run followed by an adjacent descending run forms a "run pair":

$$\tilde{R}(n_l, \tau_l) = \left\{ \tilde{R}(n_l^+, \tau_l^+), \tilde{R}(n_l^-, \tau_l^-) \right\} \tag{9}$$

where, $n_l = n_l^+$ represents the starting power frequency cycle number of the run pair, and $\tau_l = \tau_l^+ + \tau_l^-$ denotes the length of the run pair.

Definition 2: Run Ascent Height $I_r[\tilde{R}(n_l^\pm, \tau_l^\pm)]$

Let $\tilde{R}_{\max}(n_l^+, \tau_l^+)$ denote the maximum value in a run and $I_k^d(n_l^+)$ denote the amplitude at the starting point of a run, for ascending runs, the ascent height is given by:

$$I_r[\tilde{R}(n_l^\pm, \tau_l^\pm)] = I_r[\tilde{R}(n_l^+, \tau_l^+)] = \tilde{R}_{\max}(n_l^+, \tau_l^+) - I_k^d(n_l^+) \tag{10}$$

Let $\tilde{R}_{\min}(n_l^-, \tau_l^-)$ represent the minimum value and $I_k^d(n_l^- + \tau_l^-)$ represent the termination point in a run, respectively, for a descending run the ascent height is:

$$\begin{aligned} &I_r[\tilde{R}(n_l^\pm, \tau_l^\pm)] \\ &= I_r[\tilde{R}(n_l^-, \tau_l^-)] = I_k^d(n_l^- + \tau_l^-) - \tilde{R}_{\min}(n_l^-, \tau_l^-) \end{aligned} \tag{11}$$

Definition 3: Run Descent Height $I_f[\tilde{R}(n_l^\pm, \tau_l^\pm)]$

Let $\tilde{R}_{\max}(n_l^+, \tau_l^+)$ and $I_k^d(n_l^+ + \tau_l^+)$ denote the maximum value and the amplitude at a run termination point for an ascending run, respectively; $\tilde{R}_{\min}(n_l^-, \tau_l^-)$ and $I_k^d(n_l^-)$ denote the minimum value and the amplitude at the run starting point for a descending run, respectively. For an ascending run, $I_f[\tilde{R}(n_l^+, \tau_l^+)] = \tilde{R}_{\max}(n_l^+, \tau_l^+) - I_k^d(n_l^+ + \tau_l^+)$; for a descending run, $I_f[\tilde{R}(n_l^-, \tau_l^-)] = I_k^d(n_l^-) - \tilde{R}_{\min}(n_l^-, \tau_l^-)$.

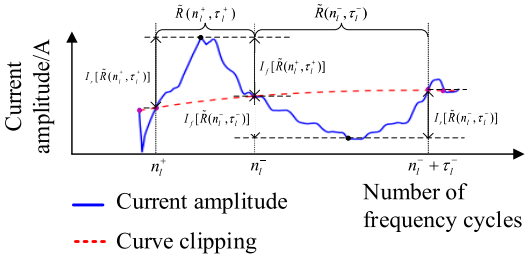

FIGURE 1. Run mapping.

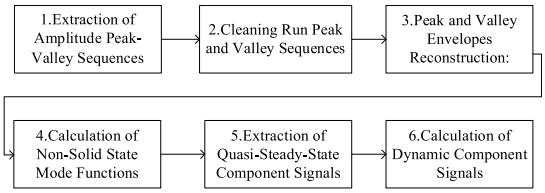

FIGURE 2. RMD method flowchart.

Using the run mapping method described in Section II-C, $I_k^d(n)$ is mapped to the run-length domain as run sequence. The run mapping, which includes concepts such as ascending runs and descending runs, is illustrated in Fig.1.

III. MODAL DECOMPOSITION METHOD IN THE RUN-LENGTH DOMAIN FOR CD ELECTRICITY SIGNALS

The run mapping requires the extraction of truncated curve $I_k^c(n)$, necessitating decomposition of complex dynamic current signals under prolonged durations. According to Cramer's theorem, a randomly fast-varying $I_k^d(n)$ can be decomposed into a slowly varying mode, referred to in this context as the quasi-steady term $I_k^m(n)$, and another rapidly fluctuating mode, termed as the dynamic term $I_k^v(n)$. The bimodal representation is expressed as:

$$I_k^d(n) = I_k^m(n) + I_k^v(n) \tag{12}$$

where, the quasi-steady term $I_k^m(n)$ serves as the amplitude parameter, utilized for the truncated curve $I_k^c(n)$ in the run mapping, simultaneously characterizing the slow fluctuation properties of signals lasting longer than 5 minutes. The dynamic term $I_k^v(n)$ represents another amplitude parameter, describing the rapid variations of the current signal in terms of local time scales, including transient (20ms-1s), short-time (1s-4s), and long-time (4s-60s) rapid changes.

This paper investigates a novel method for decomposing amplitude parameters $I_k^v(n)$ and $I_k^m(n)$ in the run-length domain, named RMD (Run-length domain Mode Decomposition). RMD method is given in Fig.2.

Meanwhile, the detailed decomposition steps of the RMD method are as follows.

Step 1: Extraction of Amplitude Peak-Valley Sequences

The current amplitude $I_k^d(n)$ is taken as an initial signal. All peak and valley sequences $\{I_k^d(n_p), I_k^d(n_v)\}, p, v = 1, 2, \ldots$ are extracted from $I_k^d(n)$ in chronological order. p, v represent the ordinal number of peaks and valleys, respectively. n_p, n_v denote the numerical value of peak and valley cycles in the power frequency cycle sequence.

TABLE 2. Function values and derivatives on subintervals.

Interpolation nodes n_l	n_0	n_1
Function values $I^d_{kP}(n_l)=y_l$	y_0	y_1
Derivative values $(I^d_{kP})'(n_l)=m_l$	m_0	m_1

Step 2: Cleaning Algorithm for Run Peak and Valley Sequences

Firstly, for the peak sequence $I^d_k(n_p)$ and valley sequence $I^d_k(n_v)$, the convexity $H(n_p)$ and concavity $H(n_v)$ of the current amplitude run peaks and valleys are defined as follows:

$$\begin{cases} H(n_p) = \left| I^d_k(n_p) - \max(I^d_k(n_v), I^d_k(n_{(v+1)})) \right| : \\ n_v < n_p < n_{(v+1)} \\ H(n_v) = \left| \min(I^d_k(n_p), I^d_k(n_{(p+1)})) - I^d_k(n_v) \right| : \\ n_p < n_v < n_{(p+1)} \end{cases} \tag{13}$$

Then, set the constants $\mathrm{H}_{p\min}$ for convexity and $\mathrm{H}_{v\min}$ for concavity. Clean the $\{I^d_k(n_p), I^d_k(n_v)\}$ sequence from Step 1 as follows:

$$\begin{cases} \text{if } \left\{H(n_p) \geq \mathrm{H}_{p\min} \text{ and } (n_{p+1} - n_p > 4)\right\}; \\ I^d_k(n_p) \Rightarrow I^d_{k\mathrm{P}}(n_l); \quad l+1 \Rightarrow l \;; p+1 \Rightarrow p; \\ else \;\; p+1 \Rightarrow p; \end{cases} \tag{14}$$

$$\begin{cases} \text{if } \{H(n_v) \geq \mathrm{H}_{v\min} \text{ and } (n_{v+1} - n_v > 4)\}; \\ I^d_k(n_v) \Rightarrow I^d_{k\mathrm{V}}(n_l); \quad l+1 \Rightarrow \; l \; ; v+1 \Rightarrow v; \\ else \;\; v+1 \Rightarrow v; \;\; l \Rightarrow l; \end{cases} \tag{15}$$

where, $l = 1, 2\ldots$ represents the run sequence number. Through $I^d_k(n_p)$ and $I^d_k(n_v)$ cleaning, the peak with fluctuations greater than $\left\{\mathrm{H}_{p\min} | n_{p+1} - n_p > 4\right\}$ are retained, denoted as $I^d_{k\mathrm{P}}(n_l)$. Similarly, the valley with fluctuations greater than $\left\{\mathrm{H}_{v\min} | n_{p+1} - n_p > 4\right\}$ are retained and denoted as $I^d_{k\mathrm{V}}(n_l)$. Data cleaning can remove local minor peak fluctuations in the current run caused by noise interference.

Finally, let $I^d_{k\mathrm{P}}(n_l)$ represent the new peak sequence of runs, and let $I^d_{k\mathrm{V}}(n_l)$ represent the new valley sequence of runs, where l denotes the sequence number of ascending or descending runs.

Step 3: Interpolation and Fitting of Peak and Valley Envelopes

According to the time subintervals $[n_l, n_{l+1}]$ covered by adjacent points $I^d_{kP}(n_l)$ and $I^d_{kP}(n_{l+1})$ in the cleaned new peak sequence, compute the function values and derivative values of the two interpolation nodes $I^d_{kP}(n_l)$ and $I^d_{kP}(n_{l+1})$ for each sub-interval, as shown in the Table 2.

Let $l_p(n)$ denote the interpolation function. Construct the interpolation conditions as follows:

$$\begin{cases} l_p(n_0) = y_0, l_p(n_1) = y_1 \\ l'_p(n_0) = m_0, l'_p(n_1) = m_1 \end{cases} \tag{16}$$

Based on the interpolation conditions of nodes, function values, derivative values, and Equation (13), the Hermite interpolation algorithm is constructed as follows:

$$l_p(n) = \alpha_0(n)y_0 + \alpha_1(n)y_1 + \beta_0(n)m_0 + \beta_1(n)m_1 \tag{17}$$

TABLE 3. Interpolation polynomial parameters.

Parameters	Parameter values
$\alpha_0(n)$	$(1-2l_0'(n_0)(n-n_0))l_0^2(n)$
$\alpha_1(n)$	$(1-2l_1'(n_1)(n-n_1))l_1^2(n)$
$\beta_0(n)$	$(n-n_0))l_0^2(n)$
$\beta_1(n)$	$(n-n_1))l_1^2(n)$
$l_0(n)$	$(n-n_1)/(n_0-n_1)$
$l_0'(n)$	$1/(n_0-n_1)$
$l_1(n)$	$(n-n_0)/(n_1-n_0)$
$l_1'(n)$	$1/(n_1-n_0)$

where, the parameters of the interpolation function are as shown in Table 3.

The Hermite interpolation algorithm is employed to fit $I^d_{k\mathrm{P}}(n_l)$, resulting in the amplitude peak envelope $l_p(n)$; similarly, using the same interpolation method, $I^d_{k\mathrm{V}}(n_l)$ is fitted to obtain the amplitude trough envelope $l_v(n)$.

Step 4: Calculation of Non-Solid State Mode Functions

The non-solid state mode function is calculated by averaging $l_p(n)$ and $l_v(n)$ using the following equation:

$$l(n) = [l_p(n) + l_v(n)]/2 \tag{18}$$

If, within a 5-minute period, the amplitude of $l(n)$ satisfies the condition that the fluctuation range between adjacent maximum and minimum values exceeds 10% of the signal's rated value, then $l(n)$ is considered as the new initial signal, and steps 1 to 4 are repeated. Otherwise, the calculation of the solid-state mode function is terminated.

Step 5: Extraction of Quasi-Steady-State Component Signals

The non-solid state mode function extraction sequence, denoted as $L(n)$, is obtained by performing M-point signal extraction on $L(n)$ as follows:

$$L(n) = \begin{cases} l(n) : n = 0, M, 2M, 3M, \cdots \\ 0 \quad \text{others} \end{cases} \tag{19}$$

If the fluctuation period of the initial quasi-steady-state sequence $L(n)$ is less than 5 minutes, $L(n)$ is used instead of $I^d_{k\mathrm{P}}(n_l)$. Subsequently, Equations (13-15)'s interpolation algorithm is employed again to extract components from $L(n)$ exhibiting slow fluctuations exceeding 5 minutes as the quasi-steady-state component signal $I^m_k(n)$.

Step 6: Calculation of Dynamic Component Signals

The dynamic component signals $I^v_k(n)$ are obtained by subtracting the quasi-steady-state component $I^m_k(n)$ from the current amplitude signal $I^d_k(n)$, as follows:

$$I^v_k(n) = I^d_k(n) - I^m_k(n) \tag{20}$$

Fig. 3 shows the process of RMD method that extracts quasi-steady-state and dynamic components based on the above steps. The RMD method described above effectively decomposes CD electricity signals into two distinct components: quasi-steady-state components, characterized by slow

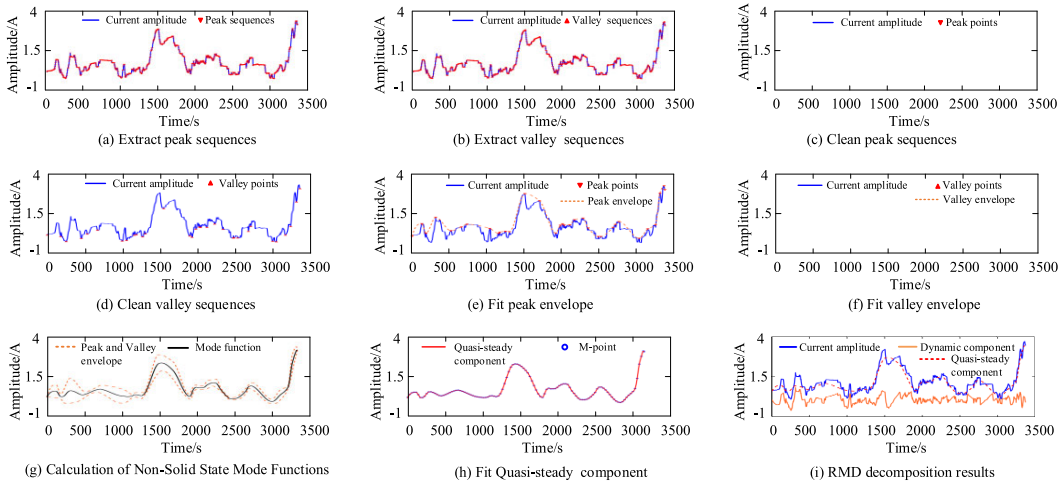

FIGURE 3. The process of RMD method.

and persistent variations over extended periods, and dynamic components, exhibiting rapid local changes over time. This approach facilitates the simultaneous extraction of both global and local characteristics of signal amplitudes. Significantly, this method represents an adaptive decomposition algorithm that does not require predefined base functions, thereby resolving the decomposition challenges associated with slow fluctuation mode $I_k^m(n)$ and rapidly changing mode $I_k^v(n)$ in complex power signals.

IV. CONSTRUCTING CHARACTERISTIC PARAMETERS AND FUNCTIONS IN RUN-LENGTH DOMAIN

In field conditions, the rapid fluctuations characteristics of CD electricity signals result in significant errors in electricity metering and therefore are termed as sensitive characteristics. It's worth noting that sensitive characteristics encompass not only the rapid changes in dynamic current amplitudes within local intervals (transient, short-time, and long-time) but also the evolution of these characteristics over prolonged periods (e.g., 60 minutes). To address the challenge of extracting sensitive characteristics, a novel method was proposed, in which two characteristic functions are constructed in the run-length domain, to analyze the characteristics of CD electricity signals within local intervals, as well as characteristics evolutionary trends. The specific method are as follows.

Definition Parameter 1: Run Pair Length τ_l

In the run-length domain, the local time length of l-th run pair, denoted as τ_l, is defined as the sum of the lengths of the ascending run τ_l^+, and the descending run τ_l^-.

Constructing the Characteristic Function 1: Run- Pair Fluctuation time length $V(l)$

Before constructing the characteristic function $V(l)$ for run pair fluctuation time, we first define an algorithm for run pair length τ_l as follows:

$$\tau_l = \text{len}[\tilde{R}(n_l^+, \tau_l^+), \tilde{R}(n_l^-, \tau_l^-)] \tag{21}$$

where, len(•) denotes the function for calculating the sequence length, and parameter τ_l has the physical meaning of the sum of the lengths of the l-th ascending and descending runs.

The fluctuation time length $V(l)$ of the run pair is used to characterize the change time of the amplitude of CD electricity signals. It is constructed by using the characteristic parameter τ_l as follows:

$$V(l) = \tau_l \times T \tag{22}$$

where, T represents power frequency cycle, and $\tau_l \times T$ signifies the time length of the run pair.

Constructing the Characteristic Function 2: Run impulse Intensity $Q(l)$

Characterizing the intensity of impulse in a current run sequence.

$$Q(l) = \frac{I_{\max}[\tilde{R}(n_l^+, n_l^+)]}{\sum_{i=1}^{10} I_i[\tilde{R}(n_l^+, n_l^+)]/10} \tag{23}$$

where, $I_{\max}[\tilde{R}(n_l^+, \tau_l^+)]$ represents the max amplitude in an ascending run, and $I_i[\tilde{R}(n_l^+, \tau_l^+)]$ represents the current amplitude at the i-th power frequency cycle within l-th run pair.

V. APPLYING RMD DECOMPOSITION AND CHARACTERISTIC EXTRACTION: CASE STUDIES

A. APPLICATION SCENARIOS

To validate the efficacy of the "run-length domain characteristic analysis theory," this study focuses on the application of photovoltaic (PV) new energy metering, aiming to analyze and extract their sensitive characteristics. The PV CD electricity signals were collected from a 110V output line of a PV substation in Zhangjiakou China. The collecting location is Metering Point II of Line Three. The power source originates from the PV power generation station. The signal sampling frequency is set at 20 kHz, with a data collection duration of 56.21 minutes.

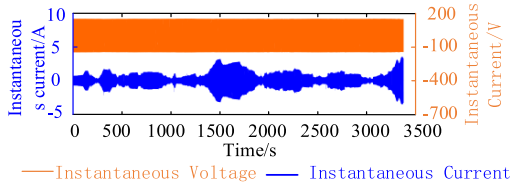

FIGURE 4. Instantaneous signal of photovoltaic A-phase voltage and current.

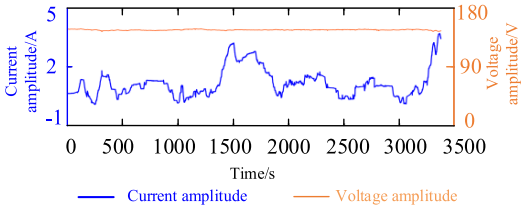

FIGURE 5. Amplitude signal of photovoltaic A-phase voltage and current.

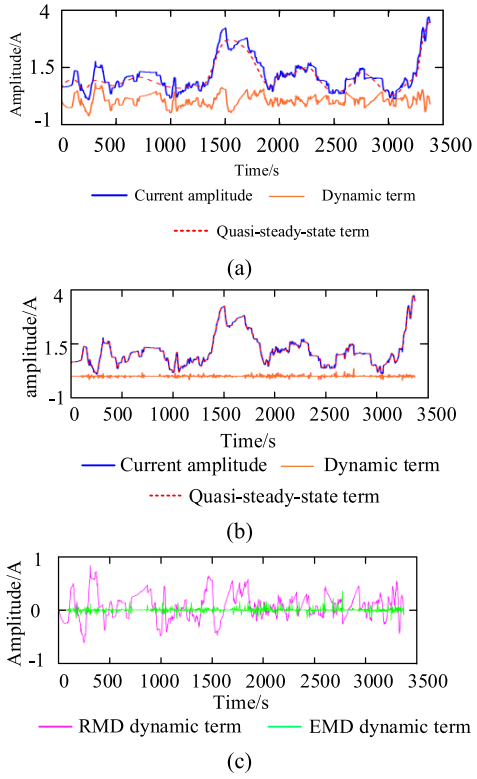

FIGURE 6. Amplitude and Metastability term signal of photovoltaic A-phase current: RMD Decomposition results (a), EMD Decomposition results (b), and their dynamic terms (c).

B. MODAL DECOMPOSITION OF CD ELECTRICITY SIGNALS IN THE RUN-LENGTH DOMAIN

In accordance with Section II-B, the instantaneous A-phase voltage and current signals are denoted as $\tilde{u}^d_{\mathrm{A}}(n')$ and $\tilde{i}^d_{\mathrm{A}}(n')$, as depicted in Fig.4. Employing the amplitude extraction method outlined in Section II-B, the fundamental voltage amplitude $U^d_{\mathrm{A}}(n)$ and current amplitude $I^d_{\mathrm{A}}(n)$ are extracted from $\tilde{u}^d_{\mathrm{A}}(n')$ and $\tilde{i}^d_{\mathrm{A}}(n')$,as illustrated in Fig.5.

For the signal $I^d_{\mathrm{A}}(n)$, modal decomposition was conducted using the aforementioned RMD method, resulting in the quasi-steady-state component signal $I^m_{\mathrm{A}}(n)$ and the dynamic component signal $I^v_{\mathrm{A}}(n)$, as depicted in Fig.6(a). To compare the differences between our proposed RMD method and the EMD (empirical mode decomposition) method, modal decomposition was also performed using the EMD method described in [18]: the residual components of the second decomposition were selected as the quasi-steady-state component, while the sum of IMF1 and IMF2 was considered as the dynamic component. The results are presented in Fig.6(b).

Analysis of the decomposition results depicted in Fig. 6(a), Fig.6(b), and Fig.6(c) reveals significant differences between the EMD and RMD methods: the quasi-steady-state component obtained by the EMD method approximates a filtering process applied to the current amplitude, resulting in a dynamic component variance of 9×10^{-4}. This indicates a loss of the wide-ranging stochastic fluctuation characteristics inherent in complex current amplitudes. In contrast, the dynamic component variance extracted by RMD is notably higher at 5.7×10^{-2}, showcasing its ability to preserve the extensive stochastic fluctuation characteristics. Moreover, the dynamic component derived from the EMD retains only transient (20 ms - 1 s) and short-time (1 s - 4 s) rapid fluctuations in the current amplitude $I^d_{\mathrm{A}}(n)$, while neglecting the long-time (4 s - 60 s) fluctuations and ultra-long-time (60 s - 300 s) fluctuations. In contrast, RMD captures transient, short-time, long-time, and ultra-long-time rapid fluctuations simultaneously. This comparison underscores the superior decomposition performance of RMD over the EMD method. In addition, Table 4 shows a comparison between these two methods.

TABLE 4. Comparison of EMD and RMD methods.

Comparison Criteria	EMD (Empirical Mode Decomposition)	RMD (Run-length domain Mode Decomposition)
Quasi-steady-state component characteristics	Approximate filtering is applied to the current amplitude	Slow and persistent variations are extracted from the current amplitude
Dynamic component variance	9.0×10^{-4}	5.7×10^{-2}
Stochastic fluctuation characteristics	Loss of extensive stochastic fluctuations	Preservation of extensive stochastic fluctuations
Transient (20 ms - 1 s) fluctuations	Captured	Captured
Short-time (1 s - 4 s) fluctuations	Captured	Captured
Long-time (4 s - 60 s) fluctuations	Neglected	Captured
Ultra-long-time (60 s - 300 s) fluctuations	Neglected	Captured

Utilizing RMD modal decomposition and further analyzing Fig.6(a), two important characteristics of dynamic load currents under photovoltaic electricity metering can be identified as follows:

Global Characteristic 1: The quasi-steady-state component signal exhibits cyclic fluctuation characteristics during long time duration.

TABLE 5. Classification and distribution proportion of current run fluctuation modes.

Run fluctuation mode classification		Length of time /s (power frequency cycles)	Run distribution proportions
Short-Time fluctuation mode		1s-4s (50-200)	13.89%
Long-Time fluctuation mode	TypeI	4s-16s (200-800)	18.06%
	TypeII	16s-60s (800-3000)	44.44%
Ultra-Long-Time fluctuation mode	TypeI	60s-180s (3000-9000)	19.44%
	TypeII	180s-300s (9000-15000)	4.17%

The quasi-steady-state component $I_{\mathrm{A}}^{m}(n)$ reflects the slow cyclic fluctuations of the current amplitude signal, with a cycle period ranging from 80 to 650 seconds.

Global Characteristic 2: The dynamic component signal demonstrates strong, stochastic and wide-ranging rapid fluctuation characteristics during long time duration.

The fluctuation time length varies between 0.5 and 300 seconds, with a amplitude mean of 7.4×10^{-2} and a amplitude variance of 5.7×10^{-2}.

C. EXTRACTION OF SENSITIVE FEATURES IN THE RUN-LENGTH DOMAIN

Utilizing the run-length domain mapping method described in Section II-C, the quasi-steady-state component $I_{\mathrm{A}}^{m}(n)$ is selected as the truncation curve $I_{\mathrm{A}}^{c}(n)$. Subsequently, the current signal $I_{\mathrm{A}}^{d}(n)$ is mapped to the run-length domain, resulting in 72 run sequences (comprising 36 ascending runs and 36 descending runs).

Based on the run-length domain characteristic functions constructed in Section IV, a run-length domain characteristic analysis of $I_{\mathrm{A}}^{d}(n)$ is conducted. This analysis extracts three sensitive characteristics of the photovoltaic new energy current signal as follows.

Run Characteristic 1: The current run sequences exhibit multiple modes of fluctuation.

Following the classification of current run fluctuation modes as outlined in Table 4, the time lengths of all runs are computed. The results indicate that the runs of current amplitude in photovoltaic CD electricity signals display three modes of fluctuation characteristics, including Short-Time, Long-Time, and Ultra-Long-Time fluctuation. And the distribution proportions of each type of run are statistically analyzed, which are presented in the rightmost column of Table 5. The mean run lengths for Short-Time Fluctuation were 98 power frequency cycles, for Long-Time were 1023 cycles, and for Ultra-Long-Time were 5025 cycles.

Run Characteristic 2: The current amplitude runs exhibit rapid fluctuation speeds.

When calculating Characteristic Function 1 for all ascending and descending runs in photovoltaic CD electricity signals, the results show that the runs exhibit rapid fluctuation speeds. Specifically, the fastest fluctuation speed for ascending runs is 0.38 s/run, while for descending runs, it is 1.22 s/run.

TABLE 6. Dynamic electrical energy testing signal model parameters.

Setting the characteristic parameter values for the OOK testing signal:	Actual current characteristic parameter values
OOK testing signal with 3 classes of run fluctuation modes Short-Time fluctuation mode: Run length 100 (50 on 50 off) (fluctuation speed 2 s/run) Long-Time fluctuation mode: Run length 1000 (500 on 500 off) (fluctuation speed 20 s/run) Ultra-Long-Time fluctuation mode: run length 5000(4000 on 1000 off) (fluctuation speed 100 s/run) Test current l impulse intensity: $Q_{\max}^{ook}(l)=4$ (50 on 150 off)	3 classes of run fluctuation modes Short-Time fluctuation mode: run length 98 (fluctuation speed 1.96 s/run) Long-Time fluctuation mode: run length 1023 (fluctuation speed 20.46 s/run) Ultra-Long-Time fluctuation mode: run length 5025 (fluctuation speed 100.5 s/run) Max impulse intensity of current run: $Q_{\max}(l)=4.18$

Run Characteristic 3: The current amplitude runs exhibit strong impulsive characteristic.

Analyzing Characteristic Function 2 for all ascending runs in photovoltaic CD electricity signals, we found that the maximum impact intensity of the runs was 4.18. This indicates that the current runs in photovoltaic renewable energy exhibit strong impulsive characteristics.

VI. EVALUATING THE IMPACT OF SENSITIVE CHARACTERISTICS ON THE DYNAMIC ERRORS IN ELECTRICITY METERS

Based on the three sensitive characteristics of the run-length domain extracted in Section V-C, we derive dynamic OOK test signal parameters, as presented in Table 6.

Simultaneously, we establish a dynamic testing system to assess the impact of these sensitive characteristics on electricity meter errors. The testing equipment is outlined in Table 7, with experimental results provided in Table 8.

During dynamic error testing experiments, we set the test voltage to 220V, current to 5A, and power factor to 1.0. The OOK test signal parameters are configured based on Table 6, representing three modes of fluctuation characteristics: short-time, long-time, and ultra-long-time run length. These parameters reflect the fluctuation speed of actual currents. Furthermore, we set the impulse intensity of the test current signal as $Q_{\max}^{ook}(l)=4$, reflecting a maximum impulse intensity of $Q_{\max}(l)=4.18$.

To depict the evolving trend of dynamic errors, the data from Table 8 is plotted as curve in Fig.7. The results in Fig.7 reveal that, when utilizing steady-state current signals as the testing signals, the errors of Meter 1 and Meter 2 under test are observed to be 0.04% and 0.02%, respectively. These values indicate no significant deviations from the expected accuracy under steady-state conditions. However, when employing OOK dynamic current testing signals with the two run-length domain sensitive characteristics to test the meters, significant dynamic errors are detected. When run-pair fluctuation time

TABLE 7. Dynamic error testing equipment and model of electric energy meters.

Testing equipment	Equipment models and error class:
harmonic power source	PCS400.3（0.02%）
Dynamic error testing device for energy meters	HE5025（±0.01%）
Three-phase standard energy meter	RD-31 Dytronic（0.01%）
Meter 1 under test	Three-phase four-wire prepayment energy meter（0.2%）
Meter 1 under test	Three-phase four-wire prepayment energy meter（0.2%）

TABLE 8. Dynamic error test results of electric energy meters.

	Testing signal	Dynamic error of meter 1 under test	Dynamic error of meter 2 under test
OOK testing signal	Steady-state current testing signal	0.04%	0.02%
	50 on 50 off $Q_{\max}^{ook}(I)=2$	12.10%	11.57%
	500 on 500 off $Q_{\max}^{ook}(I)=2$	1.85%	1.85%
	4000 on 1000 off $Q_{\max}^{ook}(I)=1.25$	0.25%	0.23%
	50 on 150 off $Q_{\max}^{ook}(I)=4$	-15.53%	-12.14%

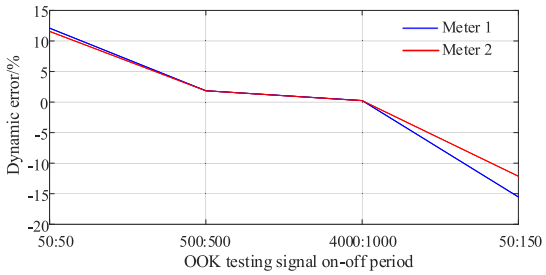

FIGURE 7. Dynamic error test results based on OOK testing signal.

length of the OOK test signal with run fluctuation mode increases from 50:50 to 50:150, the dynamic error of Meter 1 decreases from 12.10% to −15.53%, and the dynamic error of Meter 2 decreases from 11.57% to −12.14%. The testing results indicate that as the run pair length (sum of on period and off period) increases, the dynamic error of meter gradually decreases. Meanwhile, as the impulse intensity of the dynamic current testing signal increases, the meter's dynamic error also increases. The errors demonstrate the sensitivity of the proposed run-length domain characteristics, which have the potential to induce significant errors in dynamic electricity metering situations.

VII. CONCLUSION

This study focuses on representing and extracting sensitive characteristics from CD electricity metering signals to estimate their impact on electricity meter errors.

In this paper, we propose a theory for mapping CD electricity signals from the amplitude domain to the run-length domain, which involves transforming signals from the amplitude domain into run sequences in the run-length domain. We then propose a RMD (Run-Length Domain Decomposition) method to extract truncated curves in signal amplitude and decompose signals into both a slowly varying quasi-steady mode and a rapidly fluctuating dynamic mode. By comparing the RMD method with traditional EMD (Empirical Mode Decomposition) in signal decomposition, we find that the EMD method loses wide-ranging stochastic fluctuations, retaining only transient and short-time fluctuations. In contrast, the RMD method preserves extensive stochastic fluctuations and further captures long-term and ultra-long-term fluctuations. Therefore, the overall decomposition performance of the RMD method proposed in this paper is superior to that of the EMD method.

To address the extraction of sensitive characteristics that induce substantial errors in electricity metering, we construct characteristic functions and parameters in the run-length domain to facilitate the extraction of these sensitive characteristics over prolonged durations. By employing the run-length domain mapping theory and analyzing characteristic functions in the run-length domain for photovoltaic CD electricity metering signals, we identify three sensitive Run Characteristics. For example, the current amplitude runs exhibit multiple fluctuation modes and rapid speeds, as well as strong impulsive characteristics.

Validation experiments confirm the impact of these sensitive Run Characteristics on electricity meter errors. The error induced by current impulse intensity can reach up to −15.53%, while the error induced by multiple fluctuation modes and rapid speeds can reach up to 12.10%. The testing results indicate that both run pair length and impulse intensity are two key sensitive characteristics to affect the dynamic error of the electricity meter.

These findings on sensitive run characteristics will provide valuable insights for supplementing international electricity meter standards IEC 62052-11, particularly when considering the prevalence of new energy sources. Furthermore, future research will concentrate on synchronous testing methods for testing the dynamic error in electricity meters, aiming to propose supplementary testing approaches in accordance with IEC 62052. These findings will serve as a basis for recommending modifications to international standards.

DECLARATION OF COMPETING INTEREST

The manuscript is confirmed to be exclusively submitted to this journal and is not under consideration or published elsewhere. The authors affirm that there are no known financial or personal relationships that could have affected the findings presented in this article. No potential conflicts of interest exist related to the research, authorship, or publication of this work. (Di Wu, Shiyu Xie, and Xuewei Wang contributed equally to this article.)

REFERENCES

[1] G. Fernández, N. Galan, D. Marquina, D. Martínez, A. Sanchez, P. López, H. Bludszuweit, and J. Rueda, "Photovoltaic generation impact analysis in low voltage distribution grids," *Energies*, vol. 13, no. 17, p. 4347, Aug. 2020.

[2] G. Ren, J. Liu, J. Wan, W. Wang, F. Fang, F. Hong, and D. Yu, "Investigating the complementarity characteristics of wind and solar power for load matching based on the typical load demand in China," *IEEE Trans. Sustain. Energy*, vol. 13, no. 2, pp. 778–790, Apr. 2022.
[3] F. Leferink, "Conducted interference, challenges and interference cases," *IEEE Electromagn. Compat. Mag.*, vol. 4, no. 1, pp. 78–85, Jan. 2015.
[4] X. Wang, J. Wang, R. Yuan, and Z. Jiang, "Dynamic error testing method of electricity meters by a pseudo random distorted test signal," *Appl. Energy*, vol. 249, pp. 67–78, Sep. 2019.
[5] V. K. Jain, W. L. Collins, and D. C. Davis, "High-accuracy analog measurements via interpolated FFT," *IEEE Trans. Instrum. Meas.*, vols. IM-28, no. 2, pp. 113–122, Jun. 1979.
[6] J. Barros and R. I. Diego, "On the use of the Hanning window for harmonic analysis in the standard framework," *IEEE Trans. Power Del.*, vol. 21, no. 1, pp. 538–539, Jan. 2006.
[7] A. Ferrero, S. Salicone, and S. Toscani, "A fast, simplified frequency-domain interpolation method for the evaluation of the frequency and amplitude of spectral components," *IEEE Trans. Instrum. Meas.*, vol. 60, no. 5, pp. 1579–1587, May 2011.
[8] G. Andria, M. Savino, and A. Trotta, "Windows and interpolation algorithms to improve electrical measurement accuracy," *IEEE Trans. Instrum. Meas.*, vol. 38, no. 4, pp. 856–863, Aug. 1989.
[9] F. Zhang, Z. Geng, and W. Yuan, "The algorithm of interpolating windowed FFT for harmonic analysis of electric power system," *IEEE Trans. Power Del.*, vol. 16, no. 2, pp. 160–164, Apr. 2001.
[10] H. Wen, Z. Teng, and S. Guo, "Triangular self-convolution window with desirable sidelobe behaviors for harmonic analysis of power system," *IEEE Trans. Instrum. Meas.*, vol. 59, no. 3, pp. 543–552, Mar. 2010.
[11] W. Yao, Z. Teng, Q. Tang, and Y. Gao, "Measurement of power system harmonic based on adaptive Kaiser self-convolution window," *IET Gener., Transmiss. Distrib.*, vol. 10, no. 2, pp. 390–398, Feb. 2016.
[12] Y. Xiao, R.-X. Luo, W. Zhao, B. Jiang, S. Huang, and X. Zhang, "Fast quasi-synchronous harmonic algorithm for IEC61850 based digital energy metering devices," *Power Syst. Technol.*, vol. 42, no. 2, pp. 621–627, Feb. 2018.
[13] B. Zeng, Z. Teng, Y. Cai, S. Guo, and B. Qing, "Harmonic phasor analysis based on improved FFT algorithm," *IEEE Trans. Smart Grid*, vol. 2, no. 1, pp. 51–59, Mar. 2011.
[14] S. K. Singh, N. Sinha, A. K. Goswami, and N. Sinha, "Several variants of Kalman filter algorithm for power system harmonic estimation," *Int. J. Electr. Power Energy Syst.*, vol. 78, pp. 793–800, Jun. 2016.
[15] B. T. Have, T. Hartman, N. Moonen, and F. Leferink, "Misreadings of static energy meters due to conducted EMI caused by fast changing current," in *Proc. Joint Int. Symp. Electromagn. Compat., Sapporo Asia–Pacific Int. Symp. Electromagn. Compat. (EMC Sapporo/APEMC)*, Jun. 2019, pp. 445–448.
[16] B. t. Have, T. Hartman, N. Moonen, and F. Leferink, "Inclination of fast changing currents effect the readings of static energy meters," in *Proc. Int. Symp. Electromagn. Compat. EMC Eur.*, Sep. 2019, pp. 208–213.
[17] B. t. Have, M. A. Azpurua, T. Hartman, M. Pous, N. Moonen, F. Silva, and F. Leferink, "Estimation of static energy meter interference in waveforms obtained in on-site scenarios," *IEEE Trans. Electromagn. Compat.*, vol. 64, no. 1, pp. 19–26, Feb. 2022.
[18] M. Akil, E. Dokur, and R. Bayindir, "Smart coordination of predictive load balancing for residential electric vehicles based on EMD-Bayesian optimised LSTM," *IET Renew. Power Gener.*, vol. 16, no. 15, pp. 3216–3232, Nov. 2022.

RUIMING YUAN (Associate Member, IEEE) received the Ph.D. degree from Harbin Engineering University, China, in 2004.

His research interests include electrical measurement and measurement, electricity information collection, and intelligent electricity consumption.

WENWEN LI received the M.Eng. degree from Tsinghua University, China, in 2013.

Her research interest includes electrical measurement technology.

GUOXING WANG received the bachelor's degree from Beijing Union University, China, in 2008.

His research interest includes electrical measurement technology.

DI WU received the M.Eng. degree from Beijing University of Chemical Technology, China, in 2019, where he is currently pursuing the Ph.D. degree.

His research interest includes characteristics analysis of complex dynamic electricity signals.

SHIYU XIE received the bachelor's degree from Beijing University of Chemical Technology, China, in 2022.

His research interest includes characteristics analysis of complex dynamic electricity signals.

XUEWEI WANG received the Ph.D. degree from Harbin University of Science and Technology, China, in 2002.

He is currently a Professor and the Ph.D. Supervisor of Beijing University of Chemical Technology, China. His current research interests include characteristics analysis of complex dynamic electricity signals, industrial sensing signal processing, electric power and energy measuring theory and technology, and the IoT comprehensive energy remote meter reading systems.